Ocular Biometric Diurnal Rhythms in Emmetropic and Myopic Adults

Hannah J. Burfield, Nimesh B. Patel, and Lisa A. Ostrin

College of Optometry University of Houston, Houston, Texas, United States

Correspondence: Lisa A. Ostrin, College of Optometry, University of Houston, 4901 Calhoun Road, Houston, TX 77004, USA; lostrin@central.uh.edu.

PURPOSE. To investigate diurnal variations in anterior and posterior segment biometry and assess differences between emmetropic and myopic adults.

METHODS. Healthy subjects ($n = 42$, 23–41 years old) underwent biometry and spectral-domain optical coherence tomography imaging (SD-OCT) every 4 hours for 24 hours. Subjects were in darkness from 11:00 PM to 7:00 AM. Central corneal thickness, corneal power, anterior chamber depth, lens thickness, vitreous chamber depth, and axial length were measured. Thicknesses of the total retina, photoreceptor outer segments + RPE, photoreceptor inner segments, and choroid over a 6-mm annulus were determined.

RESULTS. All parameters except anterior chamber depth demonstrated significant diurnal variations, with no refractive error differences. Amplitude of choroid diurnal variation correlated with axial length ($P = 0.05$). Amplitude of axial length variation (35.71 ± 19.40 µm) was in antiphase to choroid variation (25.65 ± 2.01 µm, $P < 0.001$). The central 1-mm retina underwent variation of 5.03 ± 0.23 µm with a peak at 12 hours ($P < 0.001$), whereas photoreceptor outer segment + RPE thickness peaked at 4 hours and inner segment thickness peaked at 16 hours. Diurnal variations in retina and choroid were observed in the 3- and 6-mm annuli.

CONCLUSIONS. Diurnal rhythms in anterior and posterior segment biometry were observed over 24 hours in adults. Differences in baseline parameters were found between refractive error groups, and choroid diurnal variation correlated with axial length. The retina and choroid exhibited diurnal thickness variations in foveal and parafoveal regions.

Keywords: choroid, myopia, diurnal rhythm, axial length

Multiple ocular biometric parameters have been shown to vary with refractive error. In addition to increased axial length, a major factor in myopia, differences have also been reported in foveal retina thickness, choroid thickness, and biometric parameters of the anterior segment between emmetropic and myopic individuals.[1–3] Additionally, circadian rhythms of the human eye have been demonstrated in several ocular structures, including the cornea,[4,5] anterior chamber,[6,7] axial length,[8] retina,[9,10] and choroid.[11] Circadian rhythm in axial length may play a role in the control of eye growth and the development of refractive errors. Axial length increases during the day and decreases at night, and these axial length changes are accompanied by corresponding changes in choroid thickness.[8,12] Studies in animals show that the phase and amplitude of axial length and choroid thickness diurnal rhythms are altered in eyes that are developing refractive errors.[12–14] Specifically, in eyes that are growing at a decreased rate through the application of positive-powered spectacle lenses, rhythms in axial length phase-delay, while rhythms in choroid thickness phase-advance, bringing the two rhythms into phase with each other (Nickla DL, et al. *IOVS* 1996;37:ARVO Abstract 687). In eyes that are rapidly growing (developing myopia through the application of negative-powered lenses), axial length phase-advances, bringing choroid thickness and axial length patterns into exact antiphase (12 hours apart). Nickla[14] has suggested that the timing of peak choroid thickness in relation to other ocular rhythms associated with ocular growth could influence ocular growth rate.

Although diurnal variations in axial length and choroid have been well characterized in animal models, including the chick[14] and marmoset,[15] few studies have evaluated these diurnal ocular changes over a 24-hour period in healthy emmetropic and myopic adults.[16] Advances in partial coherence interferometry, optical low-coherence reflectometry, and spectral-domain optical coherence technology (SD-OCT) have enabled high-resolution imaging at the cellular level.[9,17] These techniques are noninvasive and noncontact, and can be performed without pupil dilation. Using an optical biometer based on partial coherence laser interferometry, Read et al.[7] showed that axial length undergoes a mean change of approximately 46 µm over 24 hours in young adult near-emmetropic subjects. The first evidence in humans that the choroid undergoes diurnal variations used partial coherence interferometry to demonstrate thickness changes over a 15-hour period.[18] Later, Chakraborty et al.[8] used optical low-coherence reflectometry to show that the choroid undergoes significant diurnal variation of approximately 29 µm in the subfoveal region over a 12-hour period. More recently, investigators found that the subfoveal choroid exhibits a significant diurnal variation of approximately 33.7 µm over an 8-hour period using SD-OCT,[19] and another study demonstrated that these diurnal changes in the choroid were consistent across the parafoveal region with a radius of 1.5 mm from the fovea.[20]

Diurnal changes in retina thickness in adult subjects have also been evaluated using SD-OCT; however, results have been conflicting. Previous studies have assessed retina thickness over a 10- to 12-hour time period and reported no diurnal variations in total retina thickness,[9,19,21] diurnal variations in only two quadrants for total retina thickness,[22] or diurnal variations in only the outer retina.[9] A recent study found that the macular region did not undergo diurnal thickness changes, but some quadrants of more peripheral regions underwent thickness changes across 24 hours.[16] Findings may have been limited by instrument resolution, small sample sizes, and observation periods that did not capture the full 24-hour diurnal period. The goal of this study was to investigate differences in diurnal variation in anterior and posterior segment ocular biometry over a 24-hour period in emmetropic and myopic adults, and to determine whether these changes occur in the parafoveal region, in addition to the fovea.

METHODS

Healthy adult subjects, ages 22 to 41 years, participated (mean $\pm$ SD, 27.2 $\pm$ 4.2 years, $n = 42$). Subjects provided informed consent after the purpose of the study and the risks were explained. The study was approved by the Committee for Protection of Human Subjects at the University of Houston and followed the tenets of the Declaration of Helsinki. All subjects had best-corrected visual acuity of 20/20 or better in each eye. Exclusion criteria included ocular disease and the use of melatonin or other pharmacological sleep aids. No subjects had systemic disease, such as diabetes or hypertension. Regular sleep/wake patterns were confirmed through the use of an actigraphy device (Actiwatch Spectrum; Phillips Respironics, Bend, OR, USA), worn for 1 week before the experiment. Specifically, all subjects slept for one period each night with consistent duration, bed time, and wake time across the week. No subjects traveled outside of two time zones in the month before the experiment.

Before participation, subjects underwent a screening to evaluate ocular health and determine non-cycloplegic autorefraction (WAM-5000; Grand Seiko, Tokyo, Japan). Subjects were classified as emmetropic (spherical equivalent refraction [SER] of +1.50 to −0.75) or myopic (SER < −0.75). The myopic group was further classified into mild (SER < −0.75 to −2.75 Diopters [D]), moderate (SER < −2.75 to −5.00 D), and severe (SER < −5.00 D) myopia.

Diurnal measurements were collected every 4 hours for 24 hours beginning at 8 hours and included seven time points. The 4-hour time interval was chosen to provide sufficient time points to observe diurnal rhythms while minimizing interruptions to subjects' daily activities and normal circadian rhythms. Subjects were asked to refrain from caffeine, alcohol, tobacco, and vigorous physical activity during the experiment. During the light period, subjects went about their daily activities in the building and were permitted to leave the building if desired, returning to the laboratory for measurements. Subjects remained in the laboratory overnight with all lights off from 11:00 PM to 7:00 AM the following day,[23] and were encouraged to sleep. The daytime illumination in the laboratory was 560 lux, and the nighttime illumination was <0.1 lux (LX1330B; Dr. Meter, Union City, CA, USA). For the two time points during the night (0 hours and 4 hours), a dim red light was used for navigating in the laboratory, and the brightness of instrument monitors was decreased to minimize disruptions to circadian rhythms. A previous study showed that brief periods of moderate illumination during the night did not interrupt diurnal variations;[24] it is unlikely that the dim red illumination utilized here altered natural circadian rhythms.

For time points during the light period, subjects first underwent a "choroid wash-out period" for 10 minutes to relax their accommodation and standardize the conditions under which SD-OCT images were collected. During the wash-out period, subjects viewed a television at 4 m. This step was not included for time points 5 and 6 during the dark period (0 hours and 4 hours).

All measurements were collected with subjects in a sitting position. A noncontact low-coherence optical biometer (LenStar; Haag-Streit, Köniz, Switzerland) was used to measure central corneal thickness, corneal power, anterior chamber depth, lens thickness, vitreous chamber depth, and axial length. Five measurements were recorded and averaged at each time point. Biometric measures were used to calculate lens power at each time point using Equation 1[25,26]:

$$Lens\ power = (1000n)/(0.378 * LT + VD)$$
$$-(SER/[1 - 0.014 * SER] + K)$$
$$/(1 - [ACD + 0.571 * LT]$$
$$*[SER/(1 - 0.014 * SER) + K]/[1000n]) \quad (1)$$

where $n = 1.336$ (index of refraction of aqueous and vitreous), LT = lens thickness, VD = vitreous chamber depth, SER = spherical equivalent refraction, and K = corneal power.

Ocular imaging was performed with SD-OCT (Spectralis, Heidelberg, Germany) using enhanced depth imaging mode. Two high-quality images of the back of the right eye were captured at each time point. The scan protocol included a six-line 30° radial scan centered at the fovea (Fig. 1). For noise reduction, B-scan averaging was set at 16 frames, and the first image at the first time point (8 hours) was set as the reference for each subject, with the instrument's tracking function used for subsequent imaging. Raw data (*.vol files) were exported and analyzed with custom written software in MatLab (Mathworks, Inc., Natick, MA, USA) using a semi-automated process. Data were adjusted for lateral magnification using axial length and corneal curvature. A three-surface schematic eye was constructed for each subject as described by Bennett and Rabbetts.[27,28] Individualized transverse scaling was then calculated assuming a spherical retina as previously described.[29,30] Image contrast was optimized, and the retina layers and sclera/choroid border were segmented. Retina segmentation included the internal limiting membrane, external limiting membrane, inner segment/outer segment border, and Bruch's membrane. The distance from Bruch's membrane to the internal limiting membrane was calculated as the total retina thickness. The distance from Bruch's membrane to the inner segment/outer segment border was calculated as the photoreceptor outer segment + RPE thickness. The distance from the inner segment/outer segment border to the external limiting membrane was calculated as the photoreceptor inner segment thickness. The distance from Bruch's membrane to the posterior choroid was calculated as the choroid thickness. Axial thickness for each layer was determined for 1536 points along each of the six scan lines. Data were binned into regions for the central 1-mm diameter, 3-mm annulus and 6-mm annulus, and further divided by quadrant into temporal, superior, nasal, and inferior regions, as described by the Early Treatment of Diabetic Retinopathy Study.[31,32]

To provide an estimate of within-session repeatability for SD-OCT–derived retina and choroid thickness, the central 1-mm total retina and choroid thickness for the two images collected at each subject's first time point (8 hours) were compared. The coefficient of variation was calculated, and the limits of agreement between repeated measures were determined with Bland-Altman analysis.[33]
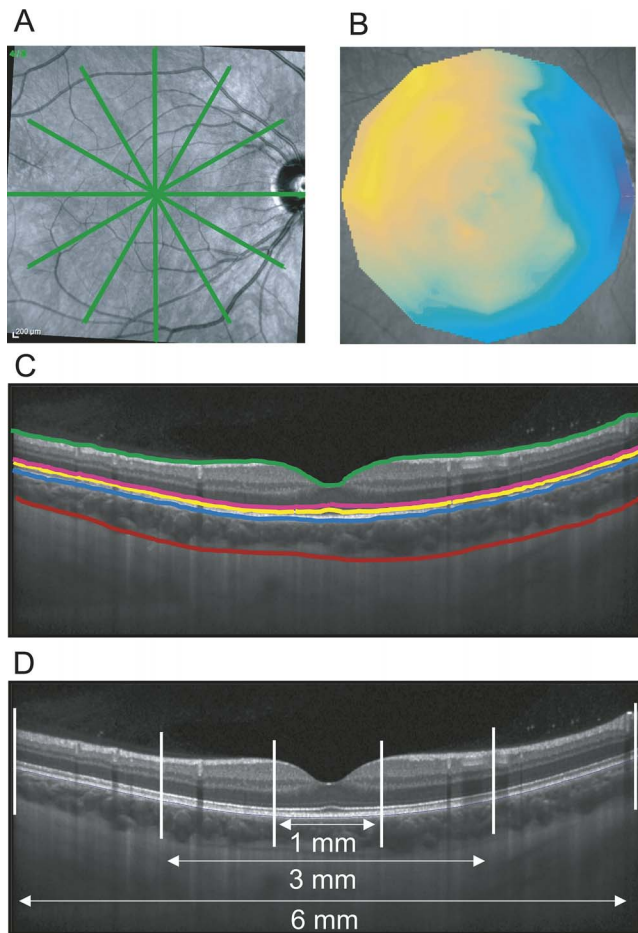
FIGURE 1. (A) Radial line scan pattern used for SD-OCT imaging. (B) Choroid thickness map generated from semi-automated segmentation. (C) Segmentation lines included the inner limiting membrane (*green*), external limiting membrane (*pink*), inner segment/outer segment junction (*yellow*), Bruch's membrane (*red*), and choroid/sclera border (*blue*). (D) Data were binned by eccentricity into the central 1-mm region, 3-mm annulus, and 6-mm annulus.

Statistical analyses were performed using MedCalc (12.3.0; MedCalc Software, Mariakerke, Belgium). Data are expressed as mean ± standard error unless otherwise noted. A critical value <0.05 is considered statistically significant. Normality was confirmed with the Shapiro-Wilk test. For each parameter, mean values for the emmetropic and myopic groups were compared with unpaired *t*-tests. For retina and choroid thickness measures, a two-factor repeated measures ANOVA was performed for refractive error (between-subjects factor) and quadrant (within-subjects factor) for 3-mm and 6-mm annuli. For analysis of diurnal measurements, data for the two 8-hour time points were averaged. Diurnal changes for each parameter were normalized to the average measurement across 24 hours for each subject, and the difference between the minimum and maximum values was calculated as the amplitude of diurnal variation. The peak (acrophase) and minimum were determined for each parameter to the nearest 4-hour time point. A two-factor repeated measures ANOVA was performed for refractive error group (between-subjects factor) and time of day (within-subjects factor) to identify significant diurnal variations and determine refractive error group differences.

Pearson correlation was used to assess differences in amplitude of axial length, retina thickness, and choroid thickness diurnal variation with SER and axial length, when treated as a continuous variable.

For axial length and subfoveal choroid thickness, circadian phase was evaluated by fitting a cosine function to the normalized data,[34,35] that is, cosinor analysis,[36] and compared for emmetropes and myopes. Other ocular and systemic measures collected in this subject population will be presented elsewhere.

RESULTS

Subject characteristics are shown in Table 1. SER of all right eyes was −2.54 ± 3.13 D and of left eyes was −2.52 ± 3.14 D. Right and left eyes were not significantly different ($P = 0.81$), and only right eyes are considered further. There were 17 subjects in the emmetropic group (SER +0.18 ± 0.55 D) and 25 subjects in the myopic group (−4.41 ± 2.75 D). Within the myopic group, there were eight mild myopes (−2.04 ± 0.56 D), nine moderate myopes (−3.83 ± 0.51 D), and nine severe myopes (−7.66 ± 2.38 D). For further analyses, all myopic subjects are grouped together.

Within-session repeatability of SD-OCT retina and choroid thickness for the central 1-mm region demonstrated coefficient of variations of 0.28% and 1.73%, respectively. Mean difference between the two retina thickness measurements was 0.003 ± 1.18 μm with limits of agreement of 2.31 μm, and between the two choroid thickness measurements was −0.96 ± 8.42 μm with limits of agreement of 16.5 μm (Fig. 2).

Refractive Error Group Differences

Refractive error group differences for the mean of each parameter are shown in Table 2. Central corneal thickness and corneal power were similar between refractive error groups ($P = 0.26$ and $P = 0.17$, respectively). Anterior chamber depth was significantly deeper in myopes compared with emmetropes ($P = 0.04$). Lens thickness and lens power were similar between refractive error groups ($P = 0.96$ and 0.61, respectively). Vitreous chamber depth and axial length were both greater in the myopic group compared with the emmetropic group ($P = 0.002$ and $P < 0.001$, respectively).

For the central 1-mm region, total retina thickness was similar between refractive error groups ($P = 0.47$, Fig. 3). Additionally, total retina thickness was similar between refractive error groups for each quadrant of the 3-mm and 6-mm annuli ($P > 0.05$ for all). On the other hand, choroid thickness in the central 1-mm region was greater in the emmetropic group (368.33 ± 17.72 μm) compared with the myopic group (305.93 ± 14.3 μm, $P = 0.009$). The choroid was also thinner in the myopic group in all quadrants of the 3-mm and 6-mm annuli ($P < 0.02$ for all), except the nasal quadrant of the 6-mm annulus ($P = 0.15$).

By eccentricity, total retina thickness for all subjects was significantly thinnest in the central 1-mm region, at 280 ± 3.28 μm, and thickest in the 3-mm annulus, at 342.08 ± 2.65 μm ($P < 0.001$). The thickness of the 6-mm annulus (296.52 ± 2.33) was between the other two regions. The outer retina layers also demonstrated significant differences with eccentricity. The photoreceptor outer segment + RPE thickness decreased from 61.93 ± 0.54 μm in the central 1-mm, to 55.94 ± 0.45 μm in the 3-mm annulus, to 53.61 ± 0.48 μm in the 6-mm annulus ($P < 0.001$). Similarly, inner segment thickness decreased from 27.20 ± 0.44 μm in the central 1-mm, to 22.75 ± 0.27 μm in the 3-mm annulus, to 21.99 ± 0.78 in the 6-mm annulus ($P <$

Investigative Ophthalmology & Visual Science

TABLE 1. Subject Demographics

	Total	Emmetropes	All Myopes	Mild Myopes	Moderate Myopes	Severe Myopes
Subjects (M/F)	42 (14/28)	17 (10/7)	25 (4/21)	9 (2/7)	8 (2/6)	8 (0/8)
Age, y	27.18 ± 4.17 (25.56, 22.37 to 41.42)	26.35 ± 2.73 (25.77, 23.02 to 32.63)	27.79 ± 4.88 (25.35, 22.37 to 41.42)	25.77 ± 2.13 (25.18, 23.44 to 30.71)	29.99 ± 6.00 (28.28, 24.33 to 41.42)	27.72 ± 5.47 (25.16, 22.37 to 38.13)
SER, D	−2.55 ± 3.13 (−1.93, +1.32 to −11.18)	+0.18 ± 0.55 (+0.19, +1.32 to −0.69)	−4.41 ± 2.75 (−3.56, −1.31 to −11.18)	−2.04 ± 0.56 (−2.00, −1.31 to −2.75)	−3.83 ± 0.51 (−3.56, −3.25 to −4.5)	−7.66 ± 2.38 (−6.78, −5.12 to −11.18)
Axial length mm	24.66 ± 1.50 (24.57, 21.69 to 29.59)	23.77 ± 1.05 (23.91, 21.69 to 25.5)	25.26 ± 1.48 (24.81, 23.17 to 29.59)	24.41 ± 1.01 (24.2, 23.17 to 25.98)	24.89 ± 0.75 (24.73, 23.95 to 26.04)	26.57 ± 1.64 (26.49, 24.63 to 29.59)

Values represent mean ± SD. The median and range are provided in parentheses.

0.001). There were no refractive error group interactions for retina thickness by eccentricity. For the choroid, the central 1 mm was the thickest region, at 336.80 ± 12.21 µm. The 3-mm and 6-mm annuli thinned with eccentricity, at 331.13 ± 11.75 µm and 306.19 ± 9.92 µm, respectively ($P < 0.001$). Additionally, the myopic group exhibited significantly thinner choroid with eccentricity ($P = 0.005$).

By quadrant, the retina was significantly thickest in the nasal quadrant and thinnest in the temporal quadrant for the 3-mm and 6-mm annuli ($P < 0.001$ for both), with no refractive error group interactions ($P = 0.61$ and 0.74, respectively). The choroid also showed significant differences by quadrant for the 3-mm and 6-mm annuli ($P < 0.001$ for both), with the superior quadrant being the thickest and the nasal quadrant being the thinnest. Additionally, the myopic group exhibited a significantly thinner choroid by quadrant than the emmetropic group for both the 3-mm annulus ($P = 0.005$) and the 6-mm annulus ($P = 0.015$).

Biometric Diurnal Rhythms

Central corneal thickness, corneal power, vitreous chamber depth, lens thickness, lens power, and axial length exhibited significant diurnal variation over the 24-hour measurement period ($P < 0.005$ for all, Table 3; Fig. 4). Variations in anterior chamber depth were not significant ($P = 0.07$). Diurnal variations were not significantly different between refractive error groups ($P > 0.05$ for all). Vitreous chamber depth and axial length increased in phase with a peak at 12 hours and minimum at 0 hours, whereas lens thickness and lens power showed a minimum during the light period (12–20 hours), and a peak at 0 hours.

Amplitude and phase information for total retina and outer retina thickness variations over 24 hours by eccentricity and quadrant, derived from SD-OCT images, are provided in Table 4. The 1-mm central retina thickness underwent significant diurnal variation of 5.05 ± 0.23 µm, with a peak at 12 hours and a minimum at 4 hours ($P < 0.001$, Fig. 5A). Total retina thickness in all quadrants of the 3-mm and 6-mm annuli underwent biphasic variation, with two peaks and two minimums throughout the day ($P < 0.001$ for all quadrants and eccentricities, Figs. 5C, 5E). For the central 1 mm, photoreceptor outer segment + RPE thickness underwent significant diurnal variation of 2.98 ± 0.29 µm, with a peak at 4 hours and minimum at 16 hours ($P < 0.001$, Fig. 5B). There were no differences in diurnal variation between refractive error groups. Additionally, the amplitude of diurnal variation in central retina thickness was not correlated with axial length (Pearson correlation 0.105, $P = 0.51$) or SER (Pearson correlation 0.002, $P = 0.99$). Inner segment thickness underwent significant diurnal variation of 3.13 ± 0.15 µm, with a peak at 16 hours and minimum at 4 hours ($P < 0.001$, Fig. 5D).

The central 1-mm choroid thickness underwent significant diurnal variation of 25.65 ± 2.01 µm ($P < 0.001$), with a peak at 4 hours and minimum at 12 hours (Table 5; Fig. 6A). All quadrants of the 3-mm and 6-mm annuli demonstrated significant diurnal variation ($P < 0.001$, Figs. 6B, 6C). There were no differences in diurnal variation of retina or choroid thickness between refractive error groups for any eccentricity or quadrant ($P > 0.05$ for all). However, the amplitude of diurnal variation of the central 1-mm choroid correlated significantly with axial length (Pearson correlation −0.311, $P = 0.05$). The amplitude did not vary with SER (Pearson correlation 0.056, $P = 0.73$).

Fitted functions for axial length and choroid thickness for the emmetropic and myopic groups are shown in Figure 7.
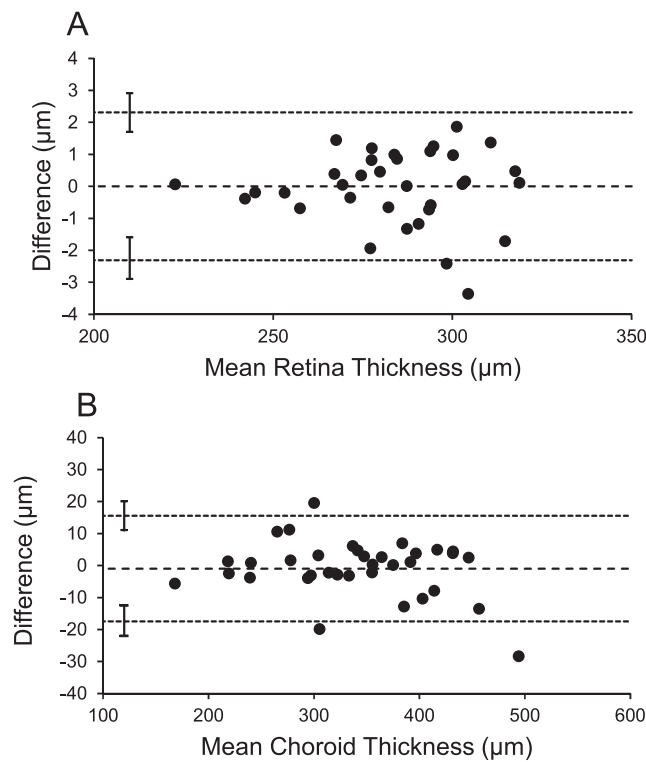
A

B

FIGURE 2. Bland-Altman analysis for repeated measures of **(A)** total retina thickness and **(B)** choroid thickness for the central 1-mm region. *Error bars* represent 95% confidence interval of the limits of agreement.[65]

DISCUSSION

Diurnal variations were observed in biometric measures of the anterior and posterior segment in healthy adult emmetropic and myopic subjects. Despite significant differences in baseline vitreous chamber depth, axial length, and choroid thickness, diurnal variations were similar between refractive error groups. However, the amplitude of diurnal variation in choroid was correlated with axial length. Variations observed in axial length and choroid thickness over 24 hours were consistent with previous studies.[8,37,38] Additionally, findings showed that significant diurnal variations in retina and choroid thickness were evident in all quadrants of the parafoveal region out to a 6-mm diameter in the posterior pole.

Diurnal variations in anterior segment biometry observed here were in accordance with previously published findings. For example, the central corneal thickness has been shown to increase during the night.[4] Evidence suggests that the closed eyelid during sleep results in a decrease in oxygen levels and

induces hypoxia, ultimately leading to an influx of water and increased corneal thickness.[39] Another study reported a significant diurnal variation in anterior chamber depth, with a peak before bedtime and a minimum on waking.[7] Although a similar amplitude and phase in anterior chamber depth variation was found here, the variation was not significant.

Few studies have examined diurnal changes in lens thickness[8] and lens power over 24 hours. Chakraborty et al.[8] examined ocular biometric measures over a 12-hour time period during 2 consecutive days, and reported no significant variation in lens thickness. On the other hand, findings presented here show a significant increase in lens thickness during the night, with an accompanying increase in lens power. Lens thickness was relatively stable during waking hours; therefore, the previous study may have not captured the diurnal variation by omitting nighttime measures. It is unclear why the lens might undergo thickening during the night. Potential factors include changes in lens metabolism that could lead to an increase in water uptake and subsequent thickening, or a change in tonus of the ciliary muscle.

Reproducibility is critically important for detecting small diurnal variations in thickness of the retina and choroid. SD-OCT has been shown to provide repeatable and precise values for retina thickness measurements.[40] Here, within-session repeatability was very high, with a coefficient of variation for total retina thickness of 0.28% and for choroid thickness of 1.73%, similar to those reported previously.[41,42] Using eye-tracking capabilities of the Spectralis SD-OCT instrument likely contributed to the high repeatability.[43] Additionally, the higher resolution and faster scanning speeds of SD-OCT compared with other imaging modalities, such as time domain OCT, also contribute to high repeatability.

Previous studies have assessed diurnal changes in retina thickness using SD-OCT. Jo et al.[21] measured total retina thickness at two time points and reported no diurnal variations. Ashraf and Nowroozzadeh[22] measured retina thickness at three time points over 12 hours and reported greater macular thickness at 7 hours only in the inferior region. Ahn et al.[16] found significant diurnal variation in total retina thickness for some regions, with no variation in outer retina thickness. Here, we measured total retina thickness, as well as photoreceptor outer segment + RPE thickness and photoreceptor inner segment thickness, over a full 24-hour period and found a significant diurnal variation of approximately 5 μm in total retina and 2 μm in outer retina layers. Read et al.[9] measured retina thickness over 10 hours and reported an approximately 5-μm diurnal variation in total retina thickness over the course of the day; however, the variation did not reach statistical significance. The authors also reported a small but significant diurnal variation in the foveal outer retina layers of 7 μm over the 10-hour period, with a peak at 13 hours.[9] Here, total retina thickness in the central 1 mm was greatest during the midday (12–16 hours) and thinnest during the night.

TABLE 2. Mean Values for Each Parameter Derived From Ocular Biometry for All Subjects ($n = 42$), Emmetropic Subjects ($n = 17$), and Myopic Subjects ($n = 25$)

Parameter	All, $n = 42$	Emmetropes, $n = 17$	Myopes, $n = 25$	P
Central corneal thickness, μm	551.78 ± 6.26	560.24 ± 9.32	545.58 ± 7.72	0.26
Corneal power, D	43.45 ± 0.25	43.44 ± 0.41	43.77 ± 0.31	0.17
Anterior chamber depth, mm	3.69 ± 0.04	3.60 ± 0.07	3.75 ± 0.04	0.04*
Lens thickness, mm	3.70 ± 0.04	3.70 ± 0.07	3.71 ± 0.05	0.96
Lens power, D	19.43 ± 0.61	21.89 ± 0.58	21.57 ± 0.32	0.61
Vitreous chamber depth, mm	17.26 ± 0.23	16.47 ± 0.25	17.43 ± 0.22	0.002*
Axial length, mm	24.66 ± 0.23	23.77 ± 0.25	25.25 ± 0.30	<0.001*

* $P < 0.05$ for unpaired *t*-test between refractive error groups is considered significant.
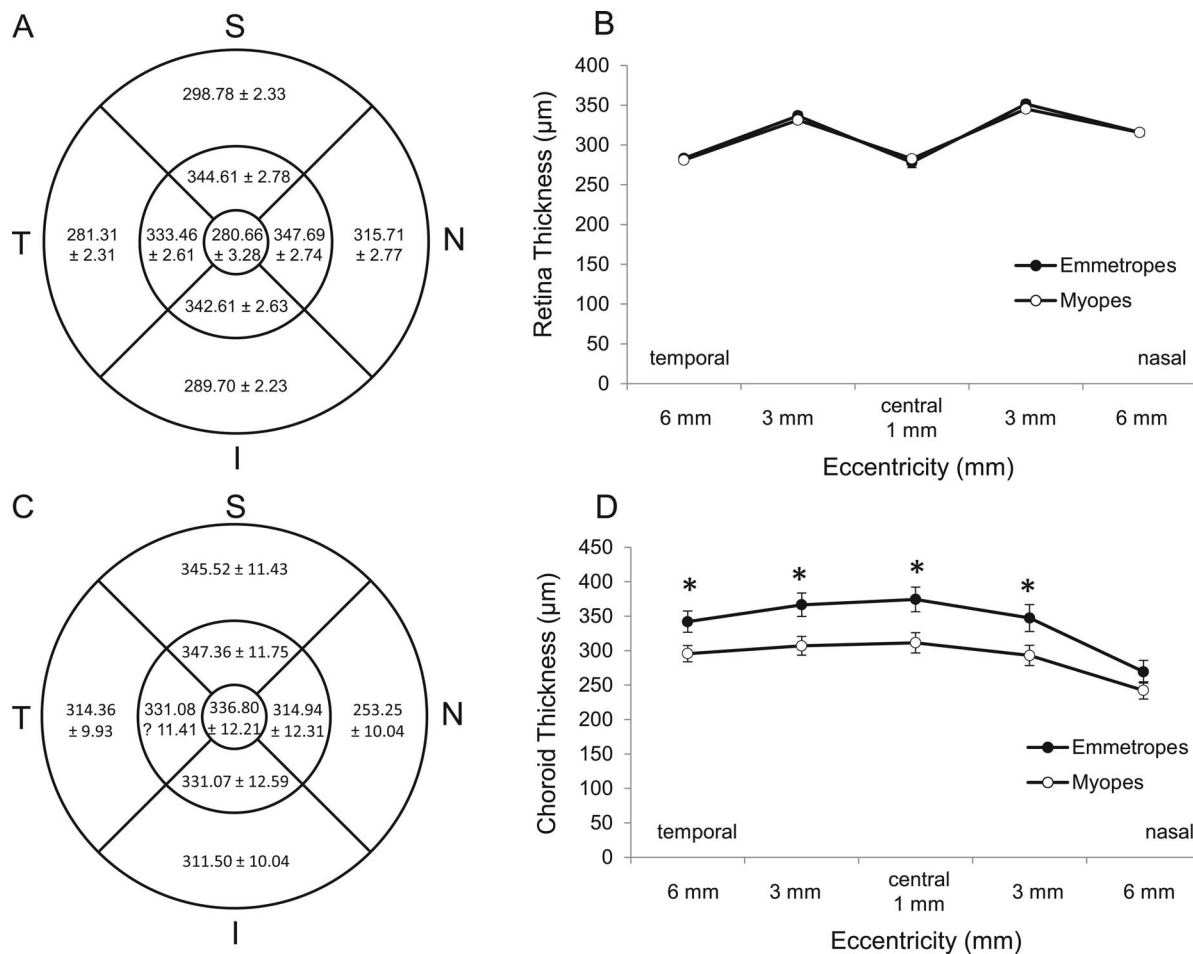
FIGURE 3. (A) Total retina thickness for all subjects by eccentricity and quadrant (mean ± SE in μm). (B) Total retinal thickness across the horizontal meridian for emmetropic subjects (closed symbols) and myopic subjects (open symbols). (C) Choroid thickness for all subjects by eccentricity and quadrant (mean ± SE in μm). (D) Choroid thickness across the horizontal meridian for emmetropic subjects (*closed symbols*) and myopic subjects (*open symbols*).

Interestingly, the diurnal variation of total retina thickness in more eccentric locations, out to the 6-mm annulus, showed a different pattern of diurnal variation that appeared biphasic, with thinning in the evening (20 hours) and also during the dark period (4 hours). Morphological differences between the central 1-mm and the 3-mm and 6-mm annuli, such as the increased length of cone photoreceptors, absence of rod photoreceptors, and absence of retinal nerve fiber layer and other inner retinal neurons at the fovea, may contribute to the regional differences in diurnal variations observed here.

The diurnal variation in the photoreceptor outer segment + RPE layer in the central 1 mm exhibited an opposite pattern to total retina thickness in the central 1 mm. The photoreceptor outer segment + RPE layer was thinnest at midday (16 hours) and thickest during the night (4 hours), with a change of approximately 2 μm throughout the 24-hour period. The photoreceptor inner segment layer was in phase with total retina thickness, being thickest at midday (16 hours) and thinnest during the night (4 hours). Photoreceptor outer segments have been shown to undergo daily renewal and

TABLE 3. Amplitude of Diurnal Change for Parameters Derived From the LenStar Biometer for All Subjects (n = 42)

Parameter	Amplitude	Time of Day Effect, P Value	Refractive Error Effect, P Value	Time by Refractive Error Interaction, P Value
Central corneal thickness	17.63 ± 1.27 μm	<0.001*	0.42	0.82
Corneal power	0.26 ± 0.02 D	<0.001*	1.0	0.46
Anterior chamber depth	95.83 ± 13.24 μm	0.07	0.42	0.19
Lens thickness	94.04 ± 13.54 μm	0.004*	0.44	0.18
Lens power	0.53 ± 0.05 D	<0.001*	1.0	0.94
Vitreous chamber depth	96.74 ± 8.56 μm	<0.001*	1.0	0.34
Axial length	35.71 ± 19.40 μm	<0.001*	1.0	0.50

P values for 2-factor repeated measures ANOVA are shown.
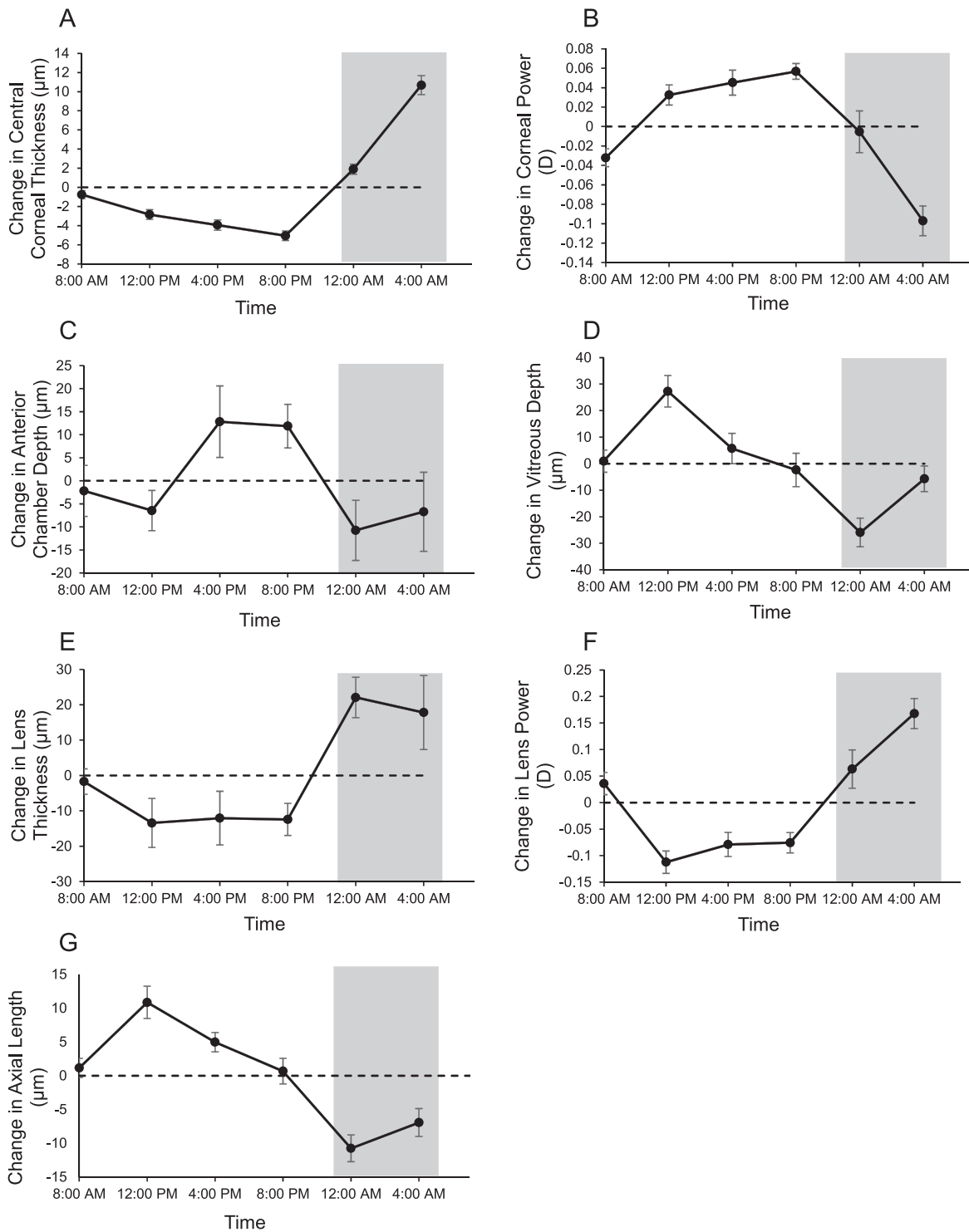* P < 0.05 considered significant.

FIGURE 4. Diurnal changes from the mean (mean ± SE) over 24 hours for all subjects for (A) central corneal thickness (μm), (B) corneal power (D), (C) anterior chamber depth (μm), (D) vitreous chamber depth (μm), (E) lens thickness (μm), (F) calculated lens power (D), and (G) axial length (μm); *shaded regions* represent the dark period.

shedding of membranous discs,[44] which helps to maintain the health of the outer retina. Early studies using ex vivo methods to examine rod and cone photoreceptor outer segment renewal rates found daily renewal rates of approximately 1 to 3 μm in mouse, dog, and Rhesus monkey eyes.[45–47] Recent studies have demonstrated this renewal process in living human eyes.[10,48,49] Using adaptive-optics OCT imaging, Ko-

caoglu et al.[10] reported an average cone outer segment length decrease of 2.1 μm. These values are similar to the daily variation in outer segment + RPE thickness of approximately 2 μm observed here.

For all subjects, the choroid was thickest in the central 1-mm region and thinned with eccentricity. Similar to findings in previous studies, regional differences also were observed.[50–52]

TABLE 4. Amplitude of Total Retina Thickness (by Eccentricity and Quadrant), Photoreceptor Outer Segment + RPE, and Photoreceptor Inner Segment (Central 1 mm) Variation Over 24 Hours

Region	Amplitude, μm	Time of Day Effect, *P* Value	Refractive Error Effect, *P* Value	Time by Refractive Error Interaction, *P* Value
Central 1-mm total retina	5.05 ± 0.23	<0.001*	0.83	0.57
Central 1-mm outer segments + RPE	2.98 ± 0.29	<0.001*	0.68	0.39
Central 1-mm inner segments	3.13 ± 0.15	<0.001*	0.31	0.15
3-mm annulus Total retina	3.48 ± 0.20	<0.001*	0.77	0.30
Temporal	3.74 ± 0.20	<0.001*	0.63	0.18
Superior	3.85 ± 0.21	<0.001*	0.84	0.53
Nasal	3.62 ± 0.21	<0.001*	0.73	0.25
Inferior	3.81 ± 0.22	<0.001*	0.92	0.42
6-mm annulus Total retina	3.17 ± 0.20	<0.001*	0.38	0.56
Temporal	3.52 ± 0.21	<0.001*	0.60	0.76
Superior	3.92 ± 0.26	<0.001*	0.42	0.74
Nasal	3.53 ± 0.16	<0.001*	0.15	0.18
Inferior	3.57 ± 0.21	<0.001*	0.68	0.48

P values for 2-factor repeated measures ANOVA are shown.
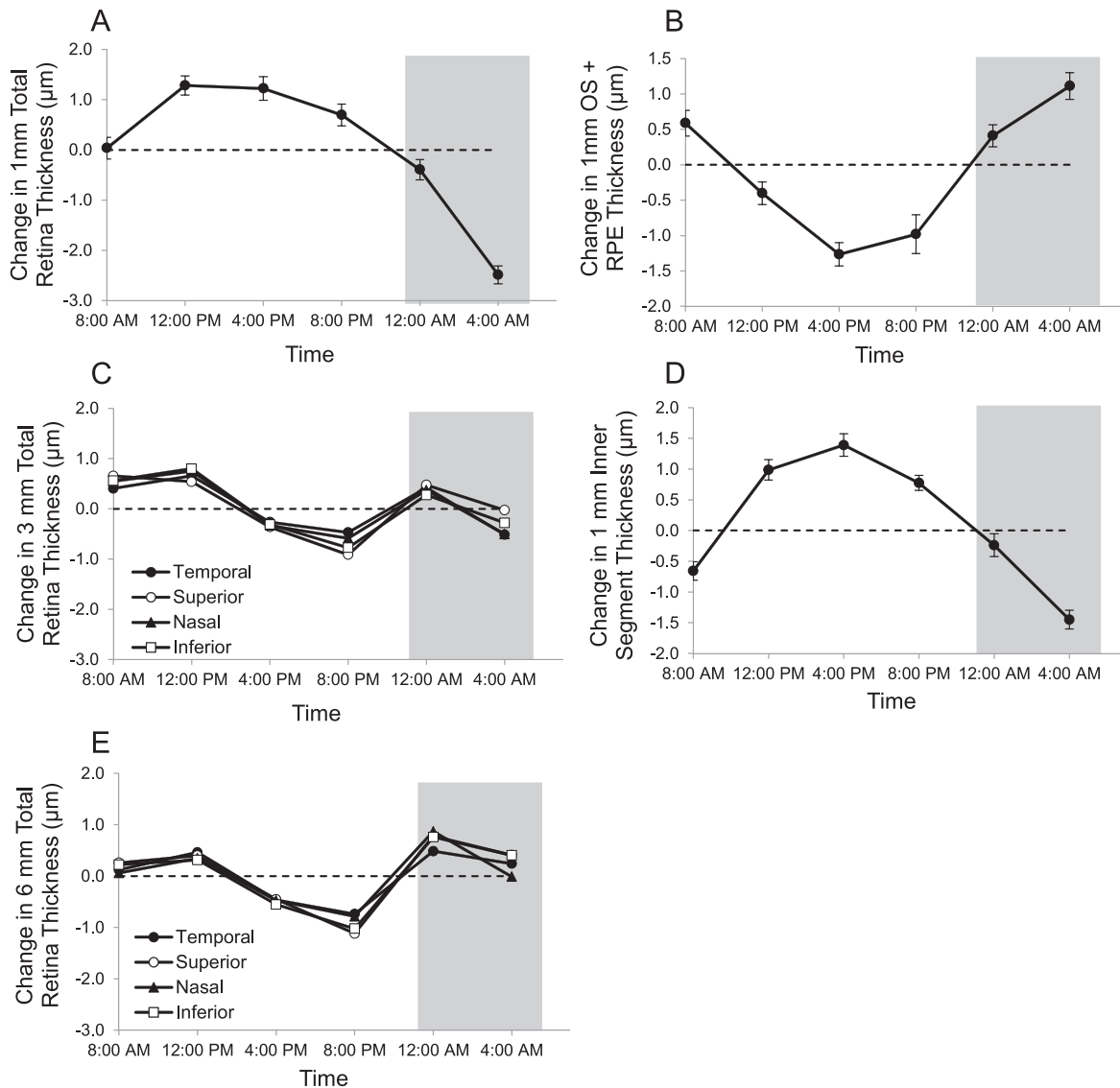* *P* < 0.05 considered significant.

FIGURE 5. Diurnal changes from the mean (mean ± SE, μm) over 24 hours for all subjects for (**A**) total retina thickness in the central 1-mm diameter, (**B**) photoreceptor outer segment (OS) + RPE thickness in the central 1-mm diameter, (**C**) total retina thickness in the 3-mm annulus by quadrant, (**D**) photoreceptor inner retina thickness in the central 1-mm diameter, and (**E**) total retina thickness in the 6-mm annulus by quadrant; *shaded regions* represent the dark period.

TABLE 5. Amplitude of Choroid Thickness Variation Over 24 Hours by Eccentricity and Quadrant

Region	Amplitude, μm	Time of Day Effect, *P* Value	Refractive Error Effect, *P* Value	Time by Refractive Error Interaction, *P* Value
Central 1 mm	25.65 ± 2.01	<0.001*	0.43	0.21
3-mm annulus	23.47 ± 1.79	<0.001*	0.37	0.17
Temporal	25.68 ± 2.21	<0.001*	0.04	0.35
Superior	25.39 ± 1.95	<0.001*	0.71	0.32
Nasal	24.56 ± 1.55	<0.001*	0.52	0.04*
Inferior	24.81 ± 1.78	<0.001*	0.81	0.27
6-mm annulus	20.05 ± 1.30	<0.001*	0.44	0.21
Temporal	19.56 ± 1.53	<0.001*	0.19	0.62
Superior	23.82 ± 1.63	<0.001*	0.64	0.45
Nasal	21.63 ± 1.45	<0.001*	0.84	0.04*
Inferior	21.72 ± 1.43	<0.001*	0.30	0.29

P values for 2-factor repeated measures ANOVA are shown.
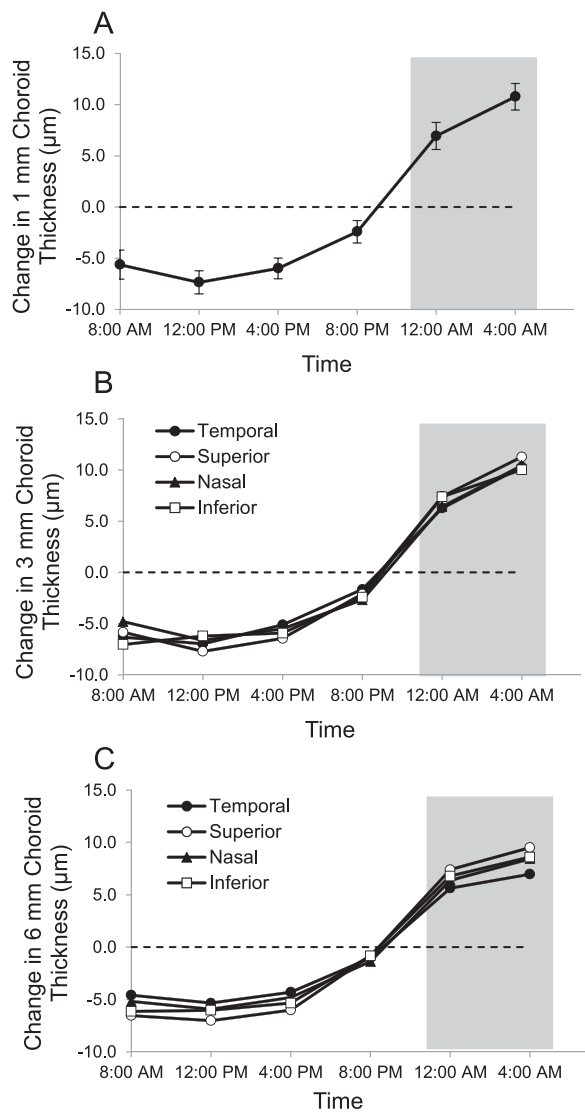* *P* < 0.05 considered significant.

FIGURE 6. Diurnal changes from the mean (mean ± SE, μm) over 24 hours for all subjects for choroid thickness in (**A**) the central 1-mm region, (**B**) the 3-mm annulus by quadrant, and (**C**) the 6-mm annulus by quadrant; *shaded regions* represent the dark period.

Specifically, the choroid was thickest in the superior quadrant and thinnest in the nasal quadrant toward the optic nerve head. Additionally, findings demonstrated that the choroid is thinner in myopic subjects compared with emmetropic subjects in all eccentricities and quadrants examined. Diurnal variations in choroid thickness were observed in the central 1-mm region and all quadrants of the 3-mm and 6-mm annuli, with a mean amplitude of 25.65 ± 2.01 μm in the central region and 23.47 ± 1.79 μm and 20.05 ± 1.30 μm in the 3-mm and 6-mm annuli, respectively. The choroid was thinnest during the light period (8 hours to 16 hours) and began to thicken at the end of the light period at 20 hours. The thickening continued during the dark period, with the thickest choroid observed at the 4-hour measurement. This diurnal pattern is similar to that observed in previous studies in humans,[8,19,53] as well as chicks[12] and marmosets.[15] Kinoshita et al.[11] showed that the change in thickness is due to an increase in luminal area, as opposed to stromal area, of the choroid.

Previous studies in animal models, including chick and marmoset, show that the relationship between axial length and choroid thickness diurnal variations is altered during myopic eye growth.[13–15,54] In agreement with previous studies in humans, our findings demonstrate that axial length and choroid thickness were in nearly exact antiphase. In this adult emmetropic and myopic population, diurnal variations were not significantly different by refractive error group. Other studies also have reported no significant differences in axial length and choroid thickness diurnal rhythms in emmetropic and myopic adults.[8] The amplitude of choroid thickness diurnal change was significantly correlated to axial length; subjects with longer axial lengths had decreased diurnal choroid thickness variation, which is similar to findings from Tan et al.,[19] in which choroid thickness was measured over a 10-hour period. These differences can be observed in the cosine fits to axial length and choroid variation between refractive error groups. For example, as seen in Figure 7, the amplitude of the fitted cosine function to axial length change over 24 hours is greater in myopes, whereas the amplitude of choroid thickness change is less in myopes. These differences could be due to a longer baseline axial length and thinner choroid in myopes, resulting in diurnal changes that are proportional to the baseline. In addition to amplitude differences, subtle phase shifts in acrophase can be observed in the fitted functions. Studies assessing younger subjects, in which myopia is still progressing, may help to clarify if
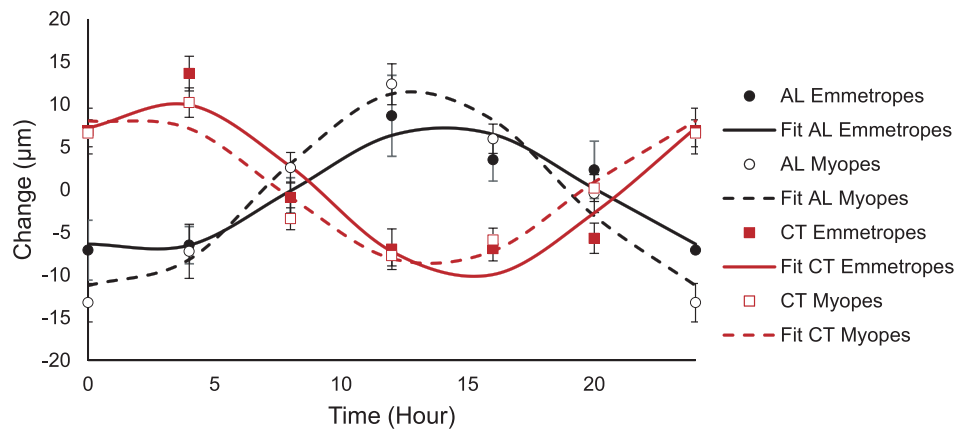
FIGURE 7. Diurnal changes from the mean (mean ± SE, μm) with fitted cosine functions over 24 hours for emmetropic subjects (*closed symbols, solid lines*) and myopic subjects (*open symbols, dashed lines*) for axial length (AL, *black lines*) and choroid thickness (*square symbols, red lines*); *shaded region* represents the dark period.

circadian changes in axial length and choroid thickness exist in human eyes actively undergoing increased growth rates.

Sleep studies can be subject to "first-night effects."[55,56] This refers to the finding that when people sleep in a new environment, alterations in sleep may occur the first night. The current experiment occurred over only one night, and therefore first-night effects may have occurred. Potential effects of altered sleep during the experiment on the retina and choroid diurnal rhythms remain unclear.

Optical methods of myopia control, such as orthokeratology and multifocal soft contact lenses, may slow myopia progression through a relative decrease in peripheral hyperopic defocus.[57–59] A study showed that contact lenses designed to reduce peripheral hyperopic defocus decreased myopia progression over 1 year by approximately one-third.[60] However, not all studies that reduce peripheral hyperopia have shown significant effects.[61] The mechanism of how peripheral defocus might slow axial elongation has yet to be elucidated. Speculation exists as to whether peripheral defocus induces thickness changes in the choroid to direct growth. In animal models, myopic defocus induces changes in choroid thickness that precede and predict the direction of eye growth, acting as an indicator of vision-dependent eye growth.[62] In humans, full-field myopic defocus has been shown to increase choroid thickness.[63,64] In these previous studies, the choroid was measured in the subfoveal region and out to 3-mm diameter in the parafoveal region. Here, we measured choroid thickness across a 30° region of the posterior pole, demonstrating that diurnal thickness changes can be seen in all quadrants out to a 6-mm diameter. Although these findings do not explain a mechanism for the effects of peripheral defocus on myopia progression, they provide evidence that the 6-mm parafoveal choroid in humans has the capacity to modulate thickness.

In conclusion, diurnal variations in multiple anterior and posterior segment biometric parameters were observed over a 24-hour period in adult emmetropic and myopic subjects. The retina and choroid exhibited diurnal thickness changes in the central 1-mm region and in all quadrants out to a 6-mm diameter in the posterior pole. Within the central 1 mm, significant diurnal variations were observed in the outer segment + RPE thickness, which were in antiphase to those observed in inner segment thickness. Choroid thickness and axial length were also in antiphase to each other. There were no significant differences in diurnal rhythms between refractive error groups for this adult population.

References

1. Fujiwara T, Imamura Y, Margolis R, Slakter JS, Spaide RF. Enhanced depth imaging optical coherence tomography of the choroid in highly myopic eyes. *Am J Ophthalmol*. 2009; 148:445–450.

2. Teberik K, Kaya M. Retinal and choroidal thickness in patients with high myopia without maculopathy. *Pak J Med Sci*. 2017; 33:1438–1443.

3. Bhardwaj V, Rajeshbhai GP. Axial length, anterior chamber depth-a study in different age groups and refractive errors. *J Clin Diagn Res*. 2013;7:2211–2212.

4. Harper CL, Boulton ME, Bennett D, et al. Diurnal variations in human corneal thickness. *Br J Ophthalmol*. 1996;80:1068–1072.

5. Read SA, Collins MJ. Diurnal variation of corneal shape and thickness. *Optom Vis Sci*. 2009;86:170–180.

6. Mapstone R, Clark CV. Diurnal variation in the dimensions of the anterior chamber. *Arch Ophthalmol*. 1985;103:1485–1486.

7. Read SA, Collins MJ, Iskander DR. Diurnal variation of axial length, intraocular pressure, and anterior eye biometrics. *Invest Ophthalmol Vis Sci*. 2008;49:2911–2918.

8. Chakraborty R, Read SA, Collins MJ. Diurnal variations in axial length, choroidal thickness, intraocular pressure, and ocular biometrics. *Invest Ophthalmol Vis Sci*. 2011;52:5121–5129.

9. Read SA, Collins MJ, Alonso-Caneiro D. Diurnal variation of retinal thickness with spectral domain OCT. *Optom Vis Sci*. 2012;89:611–619.

10. Kocaoglu OP, Liu Z, Zhang F, Kurokawa K, Jonnal RS, Miller DT. Photoreceptor disc shedding in the living human eye. *Biomed Opt Express*. 2016;7:4554–4568.

11. Kinoshita T, Mitamura Y, Shinomiya K, et al. Diurnal variations in luminal and stromal areas of choroid in normal eyes. *Br J Ophthalmol*. 2016;101:360–364.

12. Nickla DL, Wildsoet C, Wallman J. Visual influences on diurnal rhythms in ocular length and choroidal thickness in chick eyes. *Exp Eye Res*. 1998;66:163–181.

13. Papastergiou GI, Schmid GF, Riva CE, Mendel MJ, Stone RA, Laties AM. Ocular axial length and choroidal thickness in newly hatched chicks and one-year-old chickens fluctuate in a diurnal pattern that is influenced by visual experience and intraocular pressure changes. *Exp Eye Res*. 1998;66:195–205.

14. Nickla DL. The phase relationships between the diurnal rhythms in axial length and choroidal thickness and the association with ocular growth rate in chicks. *J Comp Physiol A Neuroethol Sens Neural Behav Physiol*. 2006;192:399–407.

15. Nickla DL, Wildsoet CF, Troilo D. Diurnal rhythms in intraocular pressure, axial length, and choroidal thickness in a primate model of eye growth, the common marmoset. *Invest Ophthalmol Vis Sci*. 2002;43:2519–2528.

16. Ahn J, Ahn SE, Yang KS, Kim SW, Oh J. Effects of a high level of illumination before sleep at night on chorioretinal thickness and ocular biometry. *Exp Eye Res*. 2017;164:157–167.

17. Spaide RF, Koizumi H, Pozzoni MC. Enhanced depth imaging spectral-domain optical coherence tomography. *Am J Ophthalmol*. 2008;146:496–500.

18. Brown JS, Flitcroft DI, Ying GS, et al. In vivo human choroidal thickness measurements: evidence for diurnal fluctuations. *Invest Ophthalmol Vis Sci*. 2009;50:5–12.

19. Tan CS, Ouyang Y, Ruiz H, Sadda SR. Diurnal variation of choroidal thickness in normal, healthy subjects measured by spectral domain optical coherence tomography. *Invest Ophthalmol Vis Sci*. 2012;53:261–266.

20. Chakraborty R, Read SA, Collins MJ. Hyperopic defocus and diurnal changes in human choroid and axial length. *Optom Vis Sci*. 2013;90:1187–1198.

21. Jo YJ, Heo DW, Shin YI, Kim JY. Diurnal variation of retina thickness measured with time domain and spectral domain optical coherence tomography in healthy subjects. *Invest Ophthalmol Vis Sci*. 2011;52:6497–6500.

22. Ashraf H, Nowroozzadeh MH. Diurnal variation of retinal thickness in healthy subjects. *Optom Vis Sci*. 2014;91:615–623.

23. Liu JH, Kripke DF, Twa MD, et al. Twenty-four-hour pattern of intraocular pressure in young adults with moderate to severe myopia. *Invest Ophthalmol Vis Sci*. 2002;43:2351–2355.

24. Liu JH, Kripke DF, Hoffman RE, et al. Elevation of human intraocular pressure at night under moderate illumination. *Invest Ophthalmol Vis Sci*. 1999;40:2439–2442.

25. Bennett AG. A method of determining the equivalent powers of the eye and its crystalline lens without resort to phakometry. *Ophthalmic Physiol Opt*. 1988;8:53–59.

26. Rozema JJ, Atchison DA, Tassignon MJ. Comparing methods to estimate the human lens power. *Invest Ophthalmol Vis Sci*. 2011;52:7937–7942.

27. Bennett AG, Rabbetts RB. The schematic eye. In: AG, Bennett Rabbetts RB, eds. *Clinical Visual Optics*. London: Butterworths; 1989:249–274.

28. Bennett AG, Rudnicka AR, Edgar DF. Improvements on Littmann's method of determining the size of retinal features by fundus photography. *Graefes Arch Clin Exp Ophthalmol*. 1994;232:361–367.

29. Patel NB, Wheat JL, Rodriguez A, Tran V, Harwerth RS. Agreement between retinal nerve fiber layer measures from Spectralis and Cirrus spectral domain OCT. *Optom Vis Sci*. 2012;89:E652–E666.

30. Patel NB, Garcia B, Harwerth RS. Influence of anterior segment power on the scan path and RNFL thickness using SD-OCT. *Invest Ophthalmol Vis Sci*. 2012;53:5788–5798.

31. Ohsugi H, Ikuno Y, Oshima K, Tabuchi H. 3-D choroidal thickness maps from EDI-OCT in highly myopic eyes. *Optom Vis Sci*. 2013;90:599–606.

32. Early Treatment Diabetic Retinopathy Study Research Group. Early Treatment Diabetic Retinopathy Study design and baseline patient characteristics. ETDRS report number 7. *Ophthalmology*. 1991;98:741–756.

33. Bland JM, Altman DG. Statistical methods for assessing agreement between two methods of clinical measurement. *Lancet*. 1986;1:307–310.

34. Halberg F, Reinberg A. Circadian rhythm and low frequency rhythms in human physiology [in French]. *J Physiol (Paris)*. 1967;59:117–200.

35. Refinetti R, Lissen GC, Halberg F. Procedures for numerical analysis of circadian rhythms. *Biol Rhythm Res*. 2007;38:275–325.

36. Lozano DC, Hartwick AT, Twa MD. Circadian rhythm of intraocular pressure in the adult rat. *Chronobiol Int*. 2015;32:513–523.

37. Wilson LB, Quinn GE, Ying GS, et al. The relation of axial length and intraocular pressure fluctuations in human eyes. *Invest Ophthalmol Vis Sci*. 2006;47:1778–1784.

38. Stone RA, Quinn GE, Francis EL, et al. Diurnal axial length fluctuations in human eyes. *Invest Ophthalmol Vis Sci*. 2004;45:63–70.

39. Efron N, Carney LG. Oxygen levels beneath the closed eyelid. *Invest Ophthalmol Vis Sci*. 1979;18:93–95.

40. Wolf-Schnurrbusch UE, Ceklic L, Brinkmann CK, et al. Macular thickness measurements in healthy eyes using six different optical coherence tomography instruments. *Invest Ophthalmol Vis Sci*. 2009;50:3432–3437.

41. Leung CK, Cheung CY, Weinreb RN, et al. Comparison of macular thickness measurements between time domain and spectral domain optical coherence tomography. *Invest Ophthalmol Vis Sci*. 2008;49:4893–4897.

42. Kakinoki M, Sawada O, Sawada T, Kawamura H, Ohji M. Comparison of macular thickness between Cirrus HD-OCT and Stratus OCT. *Ophthalmic Surg Lasers Imaging*. 2009;40:135–140.

43. Langenegger SJ, Funk J, Toteberg-Harms M. Reproducibility of retinal nerve fiber layer thickness measurements using the eye tracker and the retest function of Spectralis SD-OCT in glaucomatous and healthy control eyes. *Invest Ophthalmol Vis Sci*. 2011;52:3338–3344.

44. Anderson DH, Fisher SK, Steinberg RH. Mammalian cones: disc shedding, phagocytosis, and renewal. *Invest Ophthalmol Vis Sci*. 1978;17:117–133.

45. Young RW. The renewal of photoreceptor cell outer segments. *J Cell Biol*. 1967;33:61–72.

46. Buyukmihci N, Aguirre GD. Rod disc turnover in the dog. *Invest Ophthalmol*. 1976;15:579–584.

47. Anderson DH, Fisher SK, Erickson PA, Tabor GA. Rod and cone disc shedding in the rhesus monkey retina: a quantitative study. *Exp Eye Res*. 1980;30:559–574.

48. Jonnal RS, Kocaoglu OP, Wang Q, Lee S, Miller DT. Phase-sensitive imaging of the outer retina using optical coherence tomography and adaptive optics. *Biomed Opt Express*. 2012;3:104–124.

49. Jonnal RS, Besecker JR, Derby JC, et al. Imaging outer segment renewal in living human cone photoreceptors. *Opt Express*. 2010;18:5257–5270.

50. Tanabe H, Ito Y, Terasaki H. Choroid is thinner in inferior region of optic disks of normal eyes. *Retina*. 2012;32:134–139.

51. Agawa T, Miura M, Ikuno Y, et al. Choroidal thickness measurement in healthy Japanese subjects by three-dimensional high-penetration optical coherence tomography. *Graefes Arch Clin Exp Ophthalmol*. 2011;249:1485–1492.

52. Ouyang Y, Heussen FM, Mokwa N, et al. Spatial distribution of posterior pole choroidal thickness by spectral domain optical coherence tomography. *Invest Ophthalmol Vis Sci*. 2011;52:7019–7026.

53. Usui S, Ikuno Y, Akiba M, et al. Circadian changes in subfoveal choroidal thickness and the relationship with circulatory factors in healthy subjects. *Invest Ophthalmol Vis Sci*. 2012;53:2300–2307.

54. Nickla DL, Wallman J. The multifunctional choroid. *Prog Retin Eye Res*. 2010;29:144–168.

55. Tamaki M, Bang JW, Watanabe T, Sasaki Y. Night watch in one brain hemisphere during sleep associated with the first-night effect in humans. *Curr Biol*. 2016;26:1190–1194.

56. Agnew HW Jr, Webb WB, Williams RL. The first night effect: an EEG study of sleep. *Psychophysiology*. 1966;2:263–266.

57. Kang P, Swarbrick H. New perspective on myopia control with orthokeratology. *Optom Vis Sci*. 2016;93:497–503.

58. Benavente-Perez A, Nour A, Troilo D. Axial eye growth and refractive error development can be modified by exposing the peripheral retina to relative myopic or hyperopic defocus. *Invest Ophthalmol Vis Sci*. 2014;55:6765–6773.

59. Zhong Y, Chen Z, Xue F, Zhou J, Niu L, Zhou X. Corneal power change is predictive of myopia progression in orthokeratology. *Optom Vis Sci*. 2014;91:404–411.

60. Sankaridurg P, Holden B, Smith E III, et al. Decrease in rate of myopia progression with a contact lens designed to reduce relative peripheral hyperopia: one-year results. *Invest Ophthalmol Vis Sci*. 2011;52:9362–9367.

61. Sankaridurg P, Donovan L, Varnas S, et al. Spectacle lenses designed to reduce progression of myopia: 12-month results. *Optom Vis Sci*. 2010;87:631–641.

62. Hung LF, Wallman J, Smith EL III. Vision-dependent changes in the choroidal thickness of macaque monkeys. *Invest Ophthalmol Vis Sci*. 2000;41:1259–1269.

63. Chakraborty R, Read SA, Collins MJ. Monocular myopic defocus and daily changes in axial length and choroidal thickness of human eyes. *Exp Eye Res*. 2012;103:47–54.

64. Wang D, Chun RK, Liu M, et al. Optical defocus rapidly changes choroidal thickness in schoolchildren. *PLoS One*. 2016;11:e0161535.

65. Carkeet A. Exact parametric confidence intervals for Bland-Altman limits of agreement. *Optom Vis Sci*. 2015;92:e71–e80.